ChemPubSoc Europe

DOI: 10.1002/chem.201705560

CHEMISTRY A European Journal Full Paper

Fluorescent Sensors |*Hot Paper*|

Fluorescent Porous Carbazole-Decorated Copolymer Monodisperse Microspheres: Facile synthesis, Selective and Recyclable Detection of Iron (III) in Aqueous Medium

Chunyan Zhang,[a, b] Jianxin Luo,*[b] Lijuan Ou,[b] Yinghui Lun,[b] Songtao Cai,[b] Bonian Hu,[b] Guipeng Yu,*[a] and Chunyue Pan*[a]

Abstract: We demonstrate an environmentally friendly one-step soap-free emulsion polymerization strategy to develop fluorescent carbazole-based copolymer monodisperse microspheres for highly sensitive and selective detection of Fe^{3+}. The copolymer microspheres feature a stable spherical morphology with a narrow size distribution through regulating *N*-vinylcarbazole (NVCz) content (1.25–10.0 wt.%). Notably, the as-made microspheres exhibit a strong luminescence, tunable emission intensity and specific surface areas. Interestingly, the fluorescence of the copolymer microspheres can be selectively quenched by trace amounts of Fe^{3+} due to the oxidation of carbazole, and the quenching fluorescence can be facilely recovered by reduction with $NaBH_4$. Its excellent sensing performance is shown in terms of high sensitivity (low limit of detection, 1.3 μM), excellent selectivity, and rapid response rate, due to the porous nature of the copolymer microspheres. These results illustrate the copolymer microspheres obtained by simple preparative procedure without using expensive or toxic raw materials would serve as a high performance sensor for highly selective and recyclable detection of Fe^{3+} in aqueous medium.

Introduction

Iron is the most abundant transition element in living organisms, and regulates a large number of basic and essential biological processes, including oxygen metabolism, and transcriptional regulation.[1,2] Excessive iron(III) ions can cause disorders such as Alzheimer's and Parkinson's diseases.[3,4] Therefore, many efforts have been directed to develop novel efficient chemosensors for the selective recognition of Fe^{3+}.[5–14] However, most of the reported Fe^{3+} sensors always have some disadvantages, such as poor selectivity, non-renewability, limited water-solubility and biocompatibility, and sophisticated preparative procedures with using toxic or expensive raw materials. Therefore, the development of highly selective, recyclable and environmentally friendly sensors with improved sensing ability remains highly desirable.

Carbazole and its derivatives, which possess desirable photoconductivity, photosensitive, luminescence and hole- transporting properties,[15–17] have been developed as electronic materials and organic dyes for organic light-emitting diodes and photovoltaic cell.[18,19] Additionally, the polar nitrogen-rich feature enable carbazole as a novel building block for the construction of porous frameworks targeted for gas selective separation and capture extensively.[20–26] Particularly, carbazole can be oxidized chemically, providing a possibility for sensing redox-active materials. Carbazole-functionalized conjugated microporous polymer (CMP) films have be used as versatile platforms for highly sensitive and label-free chemo- and biosensing of electron-rich and electron-poor arenes, dopamine, and hypochlorous acid.[9] Interestingly, such CMP films exhibit robust reusability for the detection of Fe^{3+}. However, the reported carbazole-based CMP films/frameworks are usually fabricated using more complex preparation procedures like multistep coupling or relatively expensive raw materials including noble metal catalytic systems and halide monomers.

Depending on the synthetic procedures, morphology, and contained functionalities, polymer microspheres can be widely applied to optical displays,[27] bioimaging,[13,28–35] drug carriers,[13,28–30] adsorption materials,[36] and sensors.[13,37–41] Notably, carbazole-based polymer microspheres have emerged as promising matrices for photoelectric devices and sensors. Several polymerization approaches, including emulsion, dispersion, and suspension polymerization are available for the prepara-

[a] C. Zhang, Dr. G. Yu, Dr. C. Pan
College of Chemistry and Chemical Engineering
Hunan Provincial Key Laboratory of Efficient and Clean Utilization of Manganese Resources
Central South University, Changsha 410083 (P. R. China)
E-mail: gilbertyu@csu.edu.cn
panchunyue@csu.edu.cn

[b] C. Zhang, Dr. J. Luo, L. Ou, Y. Lun, S. Cai, B. Hu
Department of Materials and Chemical Engineering, Key Laboratory of Functional Materials for Green Building, Hunan Institute of Technology, Hengyang 421002 (P. R. China)
E-mail: luojianxin392@163.com

Supporting information and the ORCID identification number(s) for the author(s) of this article can be found under https://doi.org/10.1002/chem.201705560.

tion of polymer microspheres. In particular, soap-free emulsion polymerization without surfactants can produce surface-clean and water-dispersible monodisperse polymer microspheres, which has been used to prepare dye-containing or Eu-complexed fluorescent polymer microspheres.[35,42] However, to the best of our knowledge, fluorescent porous carbazole-based polymer microspheres prepared by soap-free emulsion polymerization of carbazole monomer (*N*-vinylcarbazole, NVCz) has not been reported until now.

In this study, novel fluorescent porous carbazole-containing copolymer monodisperse microspheres were prepared by a one-step soap-free emulsion polymerization for the first time. Styrene (St), *N*-vinylcarbazole (NVCz), methacrylic acid (MAA) and divinylbenzene (DVB) were separately selected as the matrix monomer, fluorescent monomer, water-soluble monomer and cross-linked monomer. As discussed above, carbazole may endow the copolymer microspheres with task-specific sensing properties. To be able to tune the properties of the microspheres, the growth process and influencing factors of the copolymer microspheres as well as the pores size were regulated. The relationships of composition, structure, properties, and applications of the microspheres were studied systemically. Our study provides a simple, environmentally friendly and controllable strategy to prepare copolymer microsphere for Fe^{3+} detection.

Results and Discussion

Preparation and characterization

The porous carbazole-containing copolymer microspheres were prepared through a one-step soap-free emulsion polymerization (Scheme 1). Initially, a mixture of NVCz with St and MAA was added to the aqueous phase to form oil-in-water droplets in the case of agitation. The stabilization of the droplets depends on the hydrophilic monomers (MAA).[43] A water-soluble inorganic salt such as potassium persulfate (KPS) was used as an initiator, which can be decomposed to generate anion radicals to initiate MAA to generate poly(methacrylic acid) (PMAA) oligomers. Then, hydrophobic monomers were added to the oligomers to form amphiphilic or more hydrophobic copolymers. These growing oligomers underwent *z*-mer or critical chain length for in situ micellization or precipitation, respectively, for the formation of precursor particles.[42] Meanwhile, the oligomers may act as emulsifiers for the stabilization of the precursor particles. Inadequate MAA (n-PSCz-7) is unfavourable for the stability of emulsion (Table 1). However, at high content of MAA (n-PSCz-8), the polymerization was very fast and high proportion of oligomers were generated in a short time, which leads to a rapid coagglutination and irregular aggregates.[44]

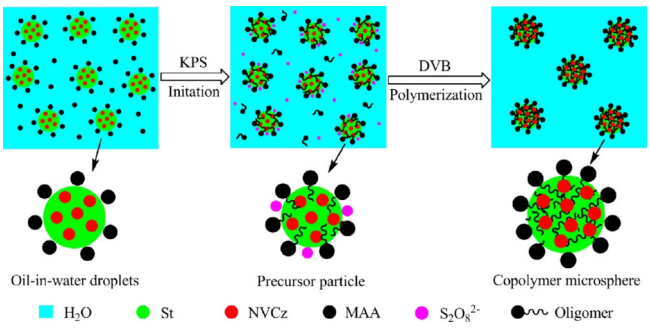

Scheme 1. Schematics for preparation route of carbazole-containing copolymer microspheres.

Table 1. Feed composition and stability of the soap-free emulsion polymerization.

Microspheres	NVCz (wt. %)[a]	[NVCz] (wt. %)[b]	MAA (wt. %)[a]	KPS (wt. %)[a]	Stability
n-PSCz-0	0	0	12.5	1.25	stable
n-PSCz-1	1.25	1.20	12.5	1.25	stable
n-PSCz-2	2.50	2.45	12.5	1.25	stable
n-PSCz-3	5.00	4.98	12.5	1.25	stable
n-PSCz-4	7.50	7.43	12.5	1.25	stable
n-PSCz-5	10.0	9.88	12.5	1.25	stable
n-PSCz-6	12.5	NA	12.5	1.25	unstable
n-PSCz-7	7.50	NA	6.25	1.25	unstable
n-PSCz-8	7.50	NA	25.0	1.25	unstable
n-PSCz-9	7.50	NA	12.5	1.00	unstable
n-PSCz-10	7.50	NA	12.5	1.88	unstable

[a] Theoretical contents calculated according to feed composition based on the amount of styrene. [b] Actual contents calculated according to elemental analyses.

In the polymerization process, the monomers transferred from the monomer droplets to the precursor particles. Consequently, the amount of droplets gradually decreased and the particles became larger. At the later stages of polymerization, excessive NVCz could be detected because of its lower reactivity than St, and then removed from monomer droplets due to its limited solubility in St. Thus, the emulsion gradually became unstable with increasing NVCz content (n-PSCz-0–n-PSCz-6), as shown in Table 1. This phenomenon was also confirmed by the morphology of the obtained copolymer microspheres (Figure 1). The copolymer microspheres with low NVCz content (<10 wt.%) had a spherical shape and a narrow size distribution. The average particle size of n-PSCz-0 was around 198 nm and it increased to 238 nm when the NVCz content is up to 10 wt.% (n-PSCz-5), as shown in Table S1. The small particle size distribution (PSD) also proves the successful generation of monodisperse copolymer microspheres. However, in the case of high NVCz content (n-PSCz-6), large particles ($d>600$ nm) and small particles ($d<200$ nm) coexisted in the polymerization system (Figure 1 (d)).

As discussed above, particle stability can be maintained with the incorporation of hydrophilic units (MAA) in the copolymer chain. The hydrophobic units were mainly located in the interior of the microspheres; on the contrary, the hydrophilic units (MAA) acted as surfactant were mainly located on the surface of the microspheres.[44] Beyond that, the carboxyl unit can also act as soluble polymer dissolved in the serum or buried in the microsphere interior. The carboxyl contents of each loci were determined (Table S1) by acid titration experiments according

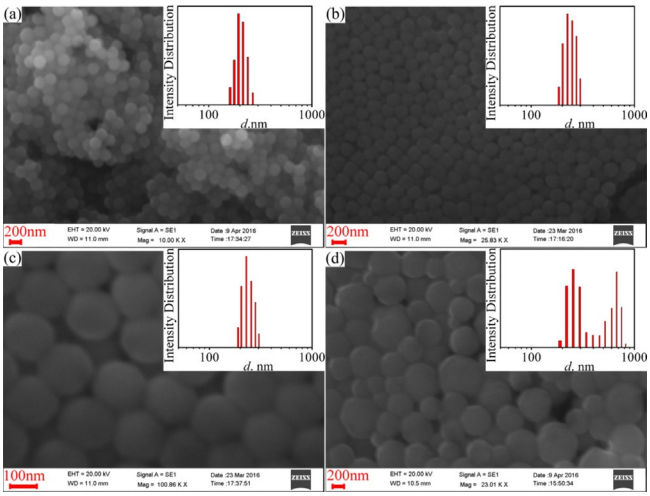

Figure 1. SEM images of the copolymer microspheres n-PSCz-0 (a), n-PSCz-4 (b), n-PSCz-5 (c) and n-PSCz-6 (d).

to the reported procedure.[45] With the increase of NVCz content, more carboxyl groups were exposed on the surface of the microspheres due to the repulsive interaction of hydrophobic NVCz. However, MAA content was fixed at 12.5 wt.% and the NVCz content increased from 0 wt.% to 12.5 wt.%. As the NVCz content increases (n-PSCz-0–n-PSCz-6), although the carboxyl content of the surface was increased, the amount of carboxyl on the surface of each microspheres decreased, which led to further aggregation of microspheres. Consequently, the average particle size (*d*) increased and the PSD broadened.

It is well known that the charge density of the microsphere surface and the ionic strength of the aqueous medium exert significant effects on the emulsion stability in soap-free emulsion polymerization.[46,47] Except for MAA, KPS can also provide electrostatic stabilization to the microspheres. The sulfate end group (SO_4^-), derived from the hydrolysis of KPS located on the surface, can enhance the electrostatic repulsive force between the microspheres; however, the ions can also compress the electric double layer of the microspheres. In other words, KPS exerted both stabilizing and destabilizing effects on the emulsion.[46] At low content of KPS (n-PSCz-9), electrostatic repulsive force originated from -SO_4^- cannot maintain the stability of the emulsion. At high KPS content (n-PSCz-10), more free radical species were produced, and consequently more precursor particles were formed. However, the content of MAA was fixed at 12.5 wt.%. Therefore, the content of carboxyl on the surface of each microsphere was low, which result in the decreasing of the stability, as shown in Table 1. Moreover, high KPS content (n-PSCz-10), similarly to high MAA content, also decreased the stability of the emulsion. This simple synthetic method can not only avoid the use of any toxic organic solvents, but also can precisely control the morphology of the microspheres by varying the contents of the monomers; consequently, stable monodisperse copolymer microspheres were prepared successfully.

The ^{13}C CP/MAS NMR spectra of typical copolymer microspheres (PSCz-0 and PSCz-4) are shown in Figure 2 and confirm

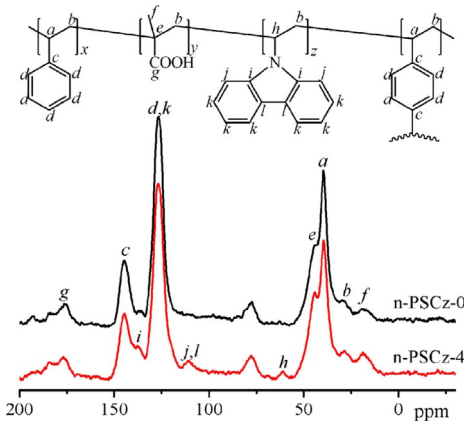

Figure 2. ^{13}C CP/MAS NMR spectra of the copolymer microspheres n-PSCz-0 and n-PSCz-4.

their chemical structure. The diagnostic chemical shifts of -CH_3 (*f*), -CH_2 (*b*) and -COOH (*g*) were located at 18, 30 and 178 ppm, respectively. Due to the difference of the substituents (phenyl, carboxyl and carbazole), the chemical shifts of -CH were located at (*a*) 38 ppm, (*e*) 42 ppm and (*h*) 63 ppm, respectively. The signals around 110–150 ppm can be attributed to phenyl and carbazole. Compared to n-PSCz-0, several characteristic peaks of carbazole appeared at (*j,l*) 112 ppm and (*i*) 137 ppm for n-PSCz-4. Figure 3 compares the FT-IR spectra of the copolymer microsphere n-PSCz-0 and n-PSCz-4. The peaks at 1696 cm^{-1} and 3450 cm^{-1} arose from C=O and O–H stretching vibration of MAA units, respectively. These peaks around 1450–1600 cm^{-1} and 700–755 cm^{-1} were assigned to the characteristic peaks of C=C and C–H in the aromatic ring. These peaks around 3000 cm^{-1} were due to asymmetrical and symmetrical stretching of -CH_3 and -CH_2. In particular, there was a new peak located at 1321 cm^{-1} associated with the characteristic absorption of C–N from carbazole.

According to the contents of various elements (C, H, and N) (Table S1), the contents of NVCz in the copolymer microspheres were calculated roughly, which were almost equal to the theoretical values as presented in Table 1. Due to steric effect of carbazole, the actual content of NVCz was slightly lower than the theoretical content. Moreover, we can find that high NVCz content leads to a large difference between the

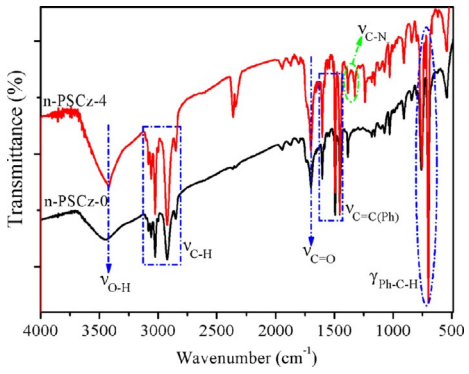

Figure 3. FT-IR spectra of the copolymer microspheres n-PSCz-0 and n-PSCz-4.

actual and the theoretical. The elements analysis together with FT-IR and ^{13}C CP/MAS NMR data indicate that the titled copolymer microspheres have been prepared successfully.

Pore properties

To characterize the porosity properties of the copolymer microspheres, nitrogen adsorption/desorption isotherm was measured at 77 K. As shown in Figure S1, the nitrogen adsorption isotherms exhibited a slight uptake in the low pressure region ($P/P_0 < 0.03$), implying a microporosity for the copolymer microspheres, whereas the isotherms also demonstrate the presence of mesopores for another relative steady rise phase ranges from 0.1 to 0.9 (P/P_0).[23,48] The rapid increase in the nitrogen sorption at a high relative pressure above 0.9 may arise partially from interparticulate porosity associated with the *meso*- and macrostructures of the samples and interparticular void.[24,25] The hysteresis between adsorption and desorption was observed for all copolymer microspheres, which is consistent with the fact that the microspheres contained both *meso*- and microporosity. The BET specific surface areas calculated from relative pressure range from 0.01 to 0.1 are listed in Table S2. n-PSCz-0 showed the lowest BET area (SA_{BET}) with a total pore volume (V_{Tot}) of 0.355 $cm^3 g^{-1}$. With the increase of NVCz content, SA_{BET} and V_{Tot} of the copolymer microspheres [n-PSCz-1 (47.7 $m^2 g^{-1}$, 0.365 $cm^3 g^{-1}$), n-PSCz-2 (57.0 $m^2 g^{-1}$, 0.428 $cm^3 g^{-1}$), n-PSCz-3 (79.4 $m^2 g^{-1}$, 0.447 $cm^3 g^{-1}$), n-PSCz-4 (93.1 $m^2 g^{-1}$, 0.459 $cm^3 g^{-1}$) and n-PSCz-5 (160.5 $m^2 g^{-1}$, 0.465 $m^3 g^{-1}$)] increased gradually.

Using nitrogen as a probe, the pore size distributions of the copolymer microspheres were obtained from the adsorption isotherms by Barret–Joyner–Halenda model. It was interesting to observe that the copolymer microspheres with selected NVCz content have tunable pore sizes. Figure S2 shows that a small fraction of pores originating from microspores and mesopores with diameter less than 20 nm for copolymer microspheres n-PSCz-0 and n-PSCz-2. A large proportion of macropores was broadly distributed from 20 to 200 nm for the two copolymer microspheres. Notably, n-PSCz-5 exhibited the highest total pore volume of 0.465 $cm^3 g^{-1}$ and the highest microporosity fraction ($V_{0.1}/V_{Tot}$) (Table S2). The micropores may be derived from the presence of carbazole and phenyl in the interior of the cross-linked microspheres due to the presence of cross-linked monomer DVB,[49] while the macropores may be originated from the gap between the microspheres. For stable monodisperse copolymer microspheres with the increase of NVCz content, the micropore volume ($V_{0.1}$) increased gradually; while the particle size became larger, which leads to large gap (macropores) between the microspheres. The porous structure endow the copolymer microspheres with large specific surface area, which may be beneficial for a fluorescence sensor due to the high-surface-area improving the contact between carbazole and analytes.[50]

Thermal properties

Figure S3 shows the DSC curves of the copolymer microspheres with various NVCz contents. All the samples showed a single glass transition temperature (T_{gd}), indicating that all monomers were randomly copolymerized. T_{gd} increased from 113 °C to 133 °C with the increase of NVCz content from 0 to 12.5 wt.%, respectively, and the results are listed in Table S3. An increase in the T_g is due to the incorporation of rigid NVCz segment (i.e., T_g of NVCz homopolymer is about 210 °C[51]). According to the Fox equation (Equation 1).

$$1/T_g = W_A/T_{gA} + W_B/T_{gB} \quad (1)$$

in which W_A is the total mass fraction of St, MAA and DVB in the copolymer microspheres; W_B is the mass fraction of NVCz in the copolymer microspheres; T_{gA} is the glass transition temperature of the copolymer microsphere n-PSCz-0; T_{gB} is the glass transition temperature of the NVCz homopolymer), the calculated glass transition temperature (T_{gc}) of the copolymer microspheres were obtained and listed in Table S3. It is clear that the calculated T_{gc} also increased with the incorporation of rigid NVCz segments. However, the rate of increasing of the calculated T_{gc} was not as fast as that of T_{gd}, which can be explained by the fact that the combination of rigid structure and crosslinking structure can promote the glass transition temperature to increase faster. Furthermore, faster heating rate of DSC measurement is also one of the reasons.

The thermal properties of the copolymer microspheres were evaluated by thermogravimetric analysis (TGA). As shown in Table S3, the temperature of 5% weight loss (T_d) for all copolymer microspheres were above 200 °C. As shown in Figure S4(a), the initial weight loss from 150 to 300 °C was related to the loss of bound water and the decarboxylation of the surface of the copolymer microspheres. The weight loss rate (W_l), as listed in Table S3, was proportional to the carboxyl content on the surface of the microspheres as listed in Table S1. With the increase of carboxyl content on the surface of microsphere, the thermal decomposition rate was accelerated and the maximum thermal decomposition temperature increased, as shown in the insert of Figure S4(b). In any case, all copolymer microspheres decomposed rapidly between 400–450 °C, and the maximum thermal decomposition temperature (T_p) were between 443–445 °C (Table S3). These thermal analysis results further confirm the chemical composition of the copolymer microspheres, and also demonstrate that the copolymer microspheres have good thermal properties for the application in the field of optoelectronics and sensors.

Photophysical properties

The absorption spectra of the water-dispersed copolymer microspheres are shown in Figure S5. All of the absorption spectra had four absorption peaks around 225, 261, 295, and 335 nm attributed to the $^1A \rightarrow {}^1C_a$, $^1A \rightarrow {}^1L_a$, $^1A \rightarrow {}^1B_a$ and $^1A \rightarrow {}^1L_b$ transition of carbazole, respectively.[51] The excitation spectra also exhibited the characteristic peaks of carbazole as shown

in Figure S6. Upon excitation with 300 nm UV light, the water-dispersed copolymer microspheres displayed two intense and overlapping emission peaks at 354 and 363 nm, which were the characteristic emissions of carbazole in the isolated state and partial overlap state, respectively.[16] As NVCz content increases, the emission spectra became diffused, that is, spectrum broadened [e.g., FWHM of n-PSCz-1, n-PSCz-2, n-PSCz-3, n-PSCz-4, and n-PSCz-5 were 40.0, 41.2, 42.1, 42.2, 44.5 nm, respectively]. A slight redshift in the λ^{fl}_{max} was observed at the maximum NVCz content in the copolymer microsphere (n-PSCz-5). These observations indicate the formation of intramolecular excimers in these copolymer microspheres with high NVCz content.[15] As NVCz content increases, the emission from the intramolecular excimers increased. This clearly suggests that the excimers were formed by the interaction of carbazole–carbazole overlap, which are located on the polymer chain and in contact with each other. In other words, the presence of comonomers in the copolymer microspheres will hinders the formation of excimers due to the steric hindrance.[15]

Consequently, the fluorescence properties of the copolymer microspheres are also dependent on NVCz contents, as shown in the insert of Figure 4 and Table S2. At a higher NVCz content

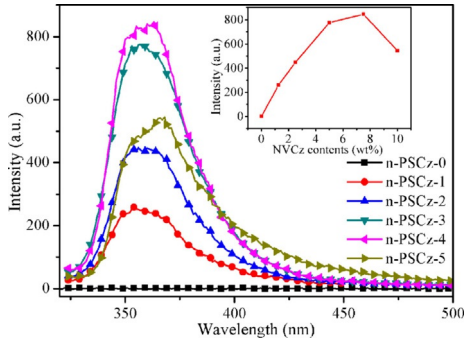

Figure 4. PL emission spectra of the water-dispersed copolymer microspheres (3 mg mL^{-1}) with different NVCz contents at excitation wavelength 300 nm. Insert of the graph illustrates the plot of the maximum intensity against vary NVCz contents.

(above 10 wt.%), the emission intensities of the copolymer microspheres decreased obviously with the increase of NVCz content. This is also due to the formation of intramolecular excimers, resulting in a certain degree of fluorescence quenching. However, at a lower NVCz content (under 10 wt.%), the PL emission intensities of the copolymer microspheres increased linearly with the increase of NVCz contents, which may be attributed to the increase of both NVCz contents and specific surface area.[50] The fluorescence quantum efficiency and fluorescence lifetime of the copolymer microspheres show a similar variation trend as the fluorescence intensity. The controllable and appropriate fluorescence properties lays the foundation for fluorescent sensing application of the copolymer microspheres.

Sensing properties

The fluorescence responses of the copolymer microspheres with different metal ions in aqueous solutions were studied. After addition of metal ions (1500 μM), we found Fe^{3+} was the strongest quencher for the copolymer microsphere n-PSCz-4 and the quenching efficiency was nearly 100% (Figure 5). How-

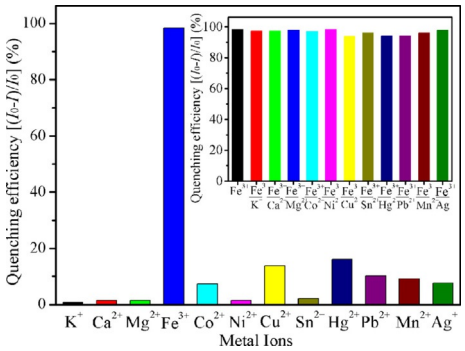

Figure 5. Fluorescence response profiles of n-PSCz-4 in aqueous solutions (2 mg mL^{-1}) upon addition of different metal ions (1500 μM). Insert of the graph illustrates fluorescence response profiles of the copolymer microsphere n-PSCz-4 in aqueous solutions upon addition of the mixture of Fe^{3+} (1500 μM) and other metal ions (1500 μM).

ever, n-PSCz-4 exhibited low sensitivity and torpid response to other metal ions. For example, the fluorescence was slightly quenched when n-PSCz-4 dispersed in an aqueous solution of other transition metals, such as Co^{2+}, Ni^{2+}, Cu^{2+}, Sn^{2+}, Hg^{2+}, Pb^{2+}, Mn^{2+} and Ag^{+}, the quenching efficiencies were less than 20%. Additionally, n-PSCz-4 was also not sensitive to alkali metal ions, such as K^{+}, Ca^{2+}, and Mg^{2+}. The potential interface due to these coexisting metal ions (K^{+}, Ca^{2+}, Mg^{2+}, Co^{2+}, Ni^{2+}, Cu^{2+}, Sn^{2+}, Hg^{2+}, Pb^{2+}, Mn^{2+} and Ag^{+}) was tested by adding these ions to the dispersion containing n-PSCz-4 and Fe^{3+}, respectively. The fluorescence intensity of the dispersion was almost equal to that of the dispersion containing only n-PSCz-4 and Fe^{3+}, as shown in the insert of Figure 5. The results clearly indicate that the copolymer microspheres showed selective detection toward Fe^{3+}, and other competitive metal ions had a low interference on Fe^{3+} fluorescence assay. In addition, the common anions such as Cl^{-}, CH_3COO^{-}, SO_4^{2-}, and NO_3^{-} showed a slight effect on Fe^{3+} detection (Figure S7), excluding the disturbance from counter anions. Therefore, we can confirm that the copolymer microspheres have promising selectivity toward Fe^{3+} detection in aqueous solutions.

To explore the sensing behaviour toward Fe^{3+}, a quantitative estimation of the quenching phenomenon of the copolymer microspheres was estimated by using fluorescence spectroscopy. It can be seen that the fluorescence intensity of the copolymer microsphere n-PSCz-4 decreased with gradual addition of Fe^{3+} (Figure 6(a)). The quenching phenomenon can be observed from micromolar to milimolar concentration of Fe^{3+}. To evaluate the sensitivity of this sensing system, we determined the Stern–Volmer quenching constant K_{SV}, which was given by the Stern–Volmer equation, $I_0/I = 1 + K_{SV}[C]$ (I_0 is the

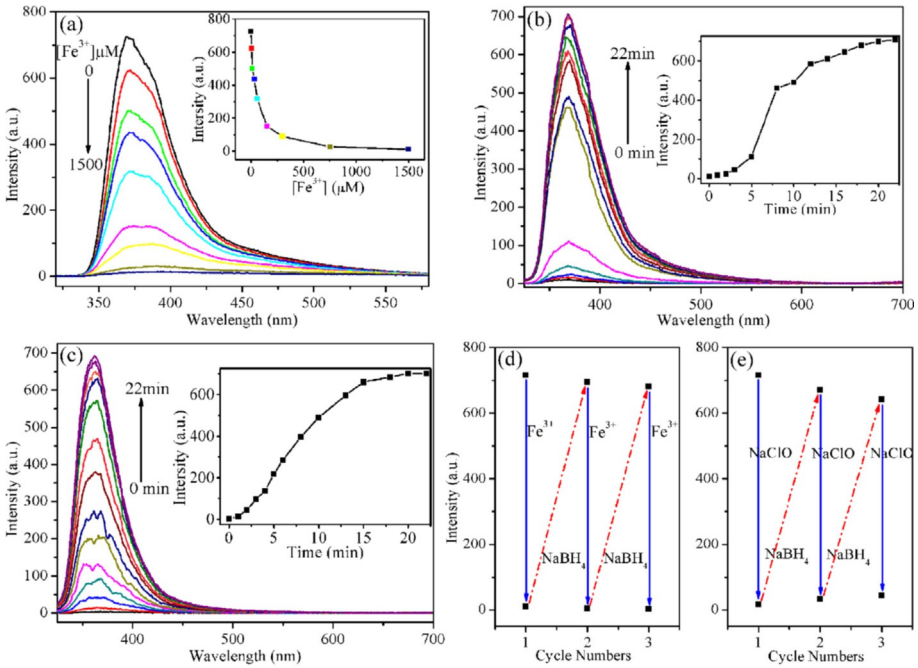

Figure 6. (a) Fluorescence response of n-PSCz-4 in aqueous solution (2 mg mL^{-1}) upon addition of Fe^{3+} (Insert: fluorescence intensity of n-PSCz-4 in aqueous solution vs. Fe^{3+} concentrations). Fluorescence response of n-PSCz-4 oxidized by 1500 μM Fe^{3+} in aqueous solution (2 mg mL^{-1}) upon addition of 2000 μM $NaBH_4$ for the first time (b) and for the second time (c) (Insert: fluorescence intensity of the mixtures of the oxidized n-PSCz-4 and $NaBH_4$ in aqueous solution vs. mixing time). Cycling test of n-PSCz-4 with 1500 μM Fe^{3+} (d) and 1500 μM NaClO (e) upon 1 min dispersion, followed by adding with 2000 μM $NaBH_4$ solution.

fluorescence intensity in the absence of the quencher, I is the fluorescence intensity after adding the quencher of concentration C, and the K_{SV} is the quenching constant of the sensors). At low concentration of Fe^{3+} (< 300 μM), I_0/I increased linearly with concentration of Fe^{3+} as shown in Figure S8. From the intercept of the fitted lines, the quenching constant K_{SV} was calculated to be 2.376×10^4 M^{-1}. The limit of detection (LOD) of Fe^{3+} with the copolymer microsphere n-PSCz-4 in aqueous medium was estimated to be 1.3 μM, which is lower than the reported Fe^{3+} sensors[7,52] and the permitted valued (5.4 μM) in drinking water by the U.S. Environmental Protection Agency (USEPA) and World Health Organization (WHO).[7] Almost total quenching of the fluorescence was achieved at 1500 μM of Fe^{3+}, and no change of emission spectra occurred with more Fe^{3+}. Thus, the tolerance level of detection of Fe^{3+} by the copolymer microsphere n-PSCz-4 in aqueous medium was 1500 μM.

At high concentrations of Fe^{3+} (> 300 μM), a positive deviation was observed, shown in the insert of Figure S8. It indicates that both static and dynamic quenching existed in the system.[52] Dynamic quenching is a kind of collisional quenching, and quenching efficiency increases with increasing temperature.[53] Figure S9 shows the temperature effect on Stern–Volmer graph. At lower Fe^{3+} concentration, the temperature has little influence on I_0/I, which indicate the quenching was mainly static. At higher Fe^{3+} concentration, I_0/I increased obviously with the increase of temperature. Figure S10 also show that the copolymer microsphere n-PSCz-4 exhibited higher quenching efficiency (I_0-I/I_0) at higher temperature. Therefore, it can be further concluded that both static quenching and dynamic quenching were effective in the fluorescence quenching of the copolymer microspheres.

It is generally known that Fe^{3+} has a standard electrode potential of 0.77 V ($E_{Fe(III)/Fe(II)}$), which is higher than the redox potential of carbazole (0.64 V).[9] When dispersing the copolymer microspheres in aqueous medium containing Fe^{3+}, the carbazole may be oxidized, leading to fluorescence quenching. In order to verify the redox-induced fluorescence quenching mechanism of the copolymer microspheres with Fe^{3+}, we monitored the corresponding changes of its fluorescence spectra when alternately mixing with $FeCl_3$ (1500 μM) and $NaBH_4$ (2000 μM) in aqueous solutions. Unsurprisingly, the emission of the copolymer microspheres quenched by Fe^{3+} was almost fully restored and the process could be repeated for at least three times (Figure 6 (b–d)). After adding Fe^{3+}, the absorption peaks of the copolymer microspheres exhibited a slightly blue-shift and relatively low absorbance (Figure S11), and the infrared spectra of the copolymer microsphere presented a new peak around 1640 cm^{-1} (Figure S12). However, all the spectra were restored to their original state after adding $NaBH_4$. These phenomenon are due to the fact that $NaBH_4$ can reduce the oxidized copolymer microspheres and recover the fluorescence, which further confirms the proposed quenching mechanism.

The time required to detect Fe^{3+} by the copolymer microsphere n-PSCz-4 has been investigated at 1500 and 60 μM, respectively (Figure S10). No significant change of fluorescence quenching efficiency was observed when tested from 0 min to 8 min at different temperature (293 K and 323 K). This suggests that the oxidation reaction between the copolymer micro-

spheres and Fe^{3+} was instantaneous, that is, the copolymer microspheres feature rapid response for Fe^{3+} by redox-induced fluorescence quenching. However, the fluorescence recovery process was time dependent. With the extension of time, the fluorescence gradually recovered, and the maximum fluorescence intensity was recovered within 22 min, as shown in Figure 6(b–c).

To further investigate the fluorescence quenching mechanism of the copolymer microsphere n-PSCz-4 with Fe^{3+}, sensing experiments of the copolymer microsphere n-PSCz-4 with other oxidants were conducted. The copolymer microsphere n-PSCz-4 exhibited a weak fluorescence quenching when mixed with $AgNO_3$ or H_2O_2 in aqueous solutions. The quenching efficiency was less than 15%, which varied with mixing time as shown in Figure S13. However, the fluorescence of the copolymer microspheres n-PSCz-4 was quenched almost completely when mixed with NaClO in aqueous solutions for only 1 min. Similarly as Fe^{3+}, NaClO can oxidize carbazole of the copolymer microspheres, leading to fluorescence quenching. Similarly, the fluorescence of the copolymer microspheres quenched by NaClO was almost fully restored by $NaBH_4$ and the process could also be repeated for at least three times (Figure 6(e)). The results show that strong oxidant can cause the fluorescence quenching of copolymer microspheres, and the reducing agent can restore the fluorescence. This further suggests that the fluorescence quenching of the copolymer microspheres was based on the oxidation of carbazole.

In order to study the influence of fluorescence intensity and porous structure on the fluorescence sensing properties of copolymer microspheres, the sensing experiments of other copolymer microspheres with Fe^{3+} were also conducted. The fluorescence intensity of n-PSCz-2 was also decreased gradually with the addition of Fe^{3+}, as shown in Figure S14. The linear correlation coefficient (R) of quenching efficiency (I_0/I) versus Fe^{3+} concentration almost reached 1 (Figure S15), indicating that fluorescence quenching effect of Fe^{3+} on n-PSCz-2 also well fits the Stern–Volmer model. The quenching constant K_{SV} and the limit of detection (LOD) were estimated as listed in Table S2. With the increase of NVCz contents, the LOD of Fe^{3+} with the copolymer microspheres decreased first and then increased. This phenomenon may be attributed to two factors. Firstly, intense fluorescence endows the copolymer microspheres with high fluorescence detection efficiency. Secondly, large specific surface area is not only favourable for the rapid transmission of iron ions in the copolymer microspheres, but also advantageous to the interaction between iron ions and carbazole; thereby improving the detection rate and detection efficiency of Fe^{3+} for the copolymer microspheres.[50,54] Compare to n-PSCz-4, the specific surface area of n-PSCz-5 increased; but the fluorescence intensity of n-PSCz-5 clearly decreased; consequently, K_{SV} of n-PSCz-5 decreased and LOD of n-PSCz-5 increased slightly. Thus, the intense fluorescence and large specific surface area ensure that the copolymer microspheres exhibit a fast detection rate and a lower detection limit for Fe^{3+} detection.

Conclusion

Novel porous carbazole-containing copolymer monodisperse microspheres were successfully prepared through a one-step soap-free emulsion polymerization. The copolymer microspheres exhibited good thermal stability, attractable BET surface areas, high luminescence intensity and excellent fluorescence sensing performance. Moreover, the PL emission intensity and specific surface area of the copolymer microspheres were tunable by varying the contents of NVCz. Particularly, the fluorescence of the copolymer microspheres could be quenched efficiently and selectively by trace Fe^{3+}. Both static quenching (redox-induced quenching) and dynamic quenching (collisional quenching) were effective in the fluorescence quench. Limit of detection (LOD) of the copolymer microspheres for Fe^{3+} in aqueous medium could as low as 1.3 μM due to intense fluorescence and large specific surface areas. Moreover, the sensing process was reversible in an aqueous medium. In summary, the titled copolymer microspheres can be obtained by simple one-step copolymerization without using expensive or toxic raw materials, which may serve as a promising sensor for the detection of Fe^{3+} in aqueous medium, with excellent selectivity, rapid response, high sensitivity and robust reusability. In addition, the relationship of structure–properties–applications may provide useful references for the future design of copolymer microspheres sensors for environmental challenges.

Acknowledgements

This work was financially supported by the National Science Foundation of China (No. 21376272 and 21674129), the Scientific Research Fund of Hunan Provincial Education Department (No.:16B064, 16C0430), Hengyang Science and Technology Project (No. 2016KG64), Hunan province college students' research learning and innovative experiment project, and the construct program of the key discipline in Hunan province.

Conflict of interest

The authors declare no conflict of interest.

Keywords: carbazole · luminescence · microsphere · porous · sensors

[1] E. Beutler, *Science* **2004**, *306*, 2051 – 2053.
[2] C. D. Kaplan, J. Kaplan, *Chem. Rev.* **2009**, *109*, 4536 – 4552.
[3] A. S. Dornelles, V. A. Garcia, M. N. M. D. Lima, G. Vedana, L. A. Alcalde, M. R. Bogo, N. Schröder, *Neurochem. Res.* **2010**, *35*, 564 – 571.
[4] A. Gaeta, R. C. Hider, *Br. J. Pharmacol.* **2009**, *146*, 1041 – 1059.
[5] S. K. Sahoo, D. Sharma, R. K. Bera, G. Crisponic, J. F. Callan, *Chem. Soc. Rev.* **2012**, *41*, 7195 – 7227.
[6] Y. Yang, X. Y. Wang, Q. L. Cui, Q. Cao, L. D. Li, *ACS Appl. Mater. Interfaces* **2016**, *8*, 7440 – 7448.
[7] A. Baral, K. Basu, S. Roy, A. Banerjee, *ACS Sustainable Chem. Eng.* **2017**, *5*, 1628 – 1637.
[8] F. Y. Gai, T. L. Zhou, Y. L. Liu, Q. S. Huo, *J. Mater. Chem. A* **2015**, *3*, 2120 – 2127.

[9] C. Gu, N. Huang, J. Gao, F. Xu, Y. H. Xu, D. L. Jiang, *Angew. Chem. Int. Ed.* **2014**, *53*, 4850 – 4855; *Angew. Chem.* **2014**, *126*, 4950 – 4955.
[10] H. Xu, J. K. Gao, X. F. Qian, J. P. Wang, H. J. He, Y. J. Cui, Y. Yang, Z. Y. Wang, G. D. Qian, *J. Mater. Chem. A* **2016**, *4*, 10900 – 10905.
[11] X. Y. Dong, R. Wang, J. Z. Wang, S. Q. Zang, T. C. W. Mak, *J. Mater. Chem. A* **2015**, *3*, 641 – 647.
[12] Z. H. Xiang, C. Q. Fang, S. H. Leng, D. P. Cao, *J. Mater. Chem. A* **2014**, *2*, 7662 – 7665.
[13] X. J. Xu, R. H. Liu, L. D. Li, *Chem. Commun.* **2015**, *51*, 16733 – 16749.
[14] J. S. Wang, X. J. Xu, L. L. Shi, L. D. Li, *ACS Appl. Mater. Interfaces* **2013**, *5*, 3392 – 3400.
[15] A. S. Brar, M. Kaur, M. M. Balamurli, S. K. Dogra, *J. Appl. Polym. Sci.* **2006**, *100*, 372 – 380.
[16] B. Liu, X. L. Yang, H. F. Ji, *Polym. Int.* **2010**, *59*, 961 – 966.
[17] J. D. Quinn, R. A. Register, *Polym. Adv. Technol.* **2008**, *19*, 556 – 559.
[18] H. Huang, Y. X. Wang, B. Pan, X. Yang, L. Wang, J. S. Chen, D. G. Ma, C. L. Yang, *Chem. Eur. J.* **2013**, *19*, 1828 – 1834.
[19] L. N. Zhu, Y. H. Shan, R. Wang, D. B. Liu, C. Zhong, Q. L. Song, F. Wu, *Chem. Eur. J.* **2017**, *23*, 4373 – 4379.
[20] Q. Chen, M. Luo, P. Hammershoj, D. Zhou, Y. Han, B. W. Laursen, C. G. Yan, B. H. Han, *J. Am. Chem. Soc.* **2012**, *134*, 6084 – 6087.
[21] Y. Liu, S. F. Wu, G. Wang, G. P. Yu, J. G. Guan, C. Y. Pan, Z. G. Wang, *J. Mater. Chem. A* **2014**, *2*, 7795 – 7801.
[22] D. Y. Chen, S. Gu, Y. Fu, Y. L. Zhu, C. Liu, G. H. Li, G. P. Yu, C. Y. Pan, *Polym. Chem.* **2016**, 7, 3416 – 3422.
[23] S. F. Wu, Y. Liu, G. P. Yu, J. G. Guan, C. Y. Pan, Y. Du, X. Xiong, Z. G. Wang, *Macromolecules* **2014**, *47*, 2875 – 2882.
[24] Q. Chen, D. P. Liu, M. Luo, L. J. Feng, Y. C. Zhao, B. H. Han, *small* **2014**, *10*, 308 – 315.
[25] C. Y. Gu, Y. Bao, W. Huang, D. Y. Liu, R. Q. Yang, *Macromol. Chem. Phys.* **2016**, *217*, 748 – 756.
[26] V. Guillerm, D. W. Kim, J. F. Eubank, R. Luebke, X. F. Liu, K. Adil, M. S. Lah, M. Eddaoudi, *Chem. Soc. Rev.* **2014**, *43*, 6141 – 6172.
[27] G. Moad, M. Chen, M. Haeussler, A. Postma, E. Rizzardo, S. H. Thang, *Polym. Chem.* **2011**, *2*, 492 – 519.
[28] M. J. Sailor, J.-H. Park, *Adv. Mater.* **2012**, *24*, 3779 – 3802.
[29] J. A. Barreto, W. O'Malley, M. Kubeil, B. Graham, H. Stephan, L. Spiccia, *Adv. Mater.* **2011**, *23*, H18 – H40.
[30] H. Zhang, J. S. Han, B. Yang, *Adv. Funct. Mater.* **2010**, *20*, 1533 – 1550.
[31] H. Y. Li, X. Q. Zhang, X. Y. Zhang, B. Yang, Y. Yang, Y. Wei, *Macromol. Rapid Commun.* **2014**, *35*, 1661 – 1667.
[32] X. M. Wang, S. P. Xu, W. Q. Xu, *Phys. Chem. Chem. Phys.* **2011**, *13*, 1560 – 1567.
[33] S. Jain, S. Chattopadhyay, R. Jackeray, C. K. V. Zainul Abid, H. Singh, *Nanoscale* **2013**, *5*, 6883 – 6892.
[34] Y. S. Wu, Y. Li, J. H. Xu, D. C. Wu, *J. Mater. Chem. B* **2014**, *2*, 5837 – 5846.
[35] H. E. Zhu, J. Tao, W. H. Wang, Y. J. Zhou, P. H. Li, Z. Li, K. Yan, S. L. Wu, K. W. K. Yeung, Z. S. Xu, H. B. Xu, P. K. Chu, *Biomaterials* **2013**, *34*, 2296 – 2306.
[36] Y. X. Xing, J. Peng, K. Xu, W. H. Lin, S. X. Gao, Y. Y. Ren, X. F. Gui, S. Y. Liang, M. C. Chen, *Chem. Eur. J.* **2016**, *22*, 2114 – 2126.
[37] J. Feng, L. Xiong, S. Q. Wang, S. Y. Li, Y. Li, G. Q. Yang, *Adv. Funct. Mater.* **2013**, *23*, 340 – 345.
[38] B. Bao, F. Y. Li, H. Li, L. F. Chen, C. Q. Ye, J. M. Zhou, J. X. Wang, Y. L. Song, L. Jiang, *J. Mater. Chem. C* **2013**, *1*, 3802 – 3807.
[39] D. Lambrechts, M. Roeffaers, G. Kerckhofs, S. J. Roberts, J. Hofkens, T. Van de Putte, H. Van Oostervvyck, J. Schrooten, *Biomaterials* **2013**, *34*, 922 – 929.
[40] A. M. Breul, M. D. Hager, U. S. Schubert, *Chem. Soc. Rev.* **2013**, *42*, 5366 – 5407.
[41] W. Ju, X. L. Song, G. Yan, K. Xu, J. Wang, D. H. Yin, L. Li, X. F. Qu, Y. G. Li, J. Li, *J. Mater. Chem. B* **2016**, *4*, 4287 – 4294.
[42] P. Govindaiah, Y. J. Jung, J. M. Lee, T.-J. Park, D. Y. Ryu, J. H. Kim, I. W. Cheong, *J. Colloid Interface Sci.* **2010**, *343*, 484 – 490.
[43] H. M. Ni, Y. Z. Du, G. H. Ma, M. Nagai, S. Omi, *Macromolecules* **2001**, *34*, 6577 – 6585.
[44] F. Wen, W. Q. Zhang, P. W. Zheng, X. Zhang, X. L. Yang, Y. Wang, X. W. Jiang, G. W. Wei, L. Q. Shi, *J. Polym. Sci. Part A* **2008**, *46*, 1192 – 1202.
[45] Y. Liang, A. I. Abdelrahman, V. Baranov, M. A. Winnik, *Polymer* **2011**, *52*, 5040 – 5052.
[46] S. Peach, *Macromolecules* **1998**, *31*, 3372 – 3373.
[47] K. Kang, C. Y. Kan, Y. Du, D. S. Liu, *Polym. Adv. Technol.* **2006**, *17*, 193 – 198.
[48] S. Kandambeth, A. Mallick, B. Lukose, M. V. Mane, T. Heine, R. Banerjee, *J. Am. Chem. Soc.* **2012**, *134*, 19524 – 19527.
[49] M. Albuszis, P. J. Roth, W. Pauer, H-U. Moritz, *Polym. Chem.* **2014**, *5*, 5689 – 5699.
[50] B. Bonillo, R. S. Sprick, A. I. Cooper, *Chem. Mater.* **2016**, *28*, 3469 – 3480.
[51] J. X. Luo, C. Y. Zhang, C. H. Li, H. X. Hua, B. N. Hu, *RSC Adv.* **2014**, *4*, 57393 – 57401.
[52] K.-W. Cha, K.-W. Park, *Talanta* **1998**, *46*, 1567 – 1571.
[53] A. Başoğlu, G. Tosun, M. Ocak, H. Alp, N. Yaylı, Ü. Ocak, *J. Agric. Food Chem.* **2015**, *63*, 2654 – 2659.
[54] Q. Zhao, M. J. Yin, A. P. Zhang, S. Prescher, M. Antonietti, J. Y. Yuan, *J. Am. Chem. Soc.* **2013**, *135*, 5549 – 5552.

Manuscript received: November 22, 2017
Accepted manuscript online: December 30, 2017
Version of record online: January 29, 2018